Multifragment Emission in Reactions Induced by 0.90 and 3.6 GeV ^{3}He Ions on ^{nat}Ag

S. J. Yennello,[1,2] E. C. Pollacco,[1] K. Kwiatkowski,[2] C. Volant,[1] R. Dayras,[1] Y. Cassagnou,[1] R. Legrain,[1] E. Norbeck,[3] V. E. Viola,[2] J. L. Wile,[2,a] and N. R. Yoder[2]

[1]*Département de Physique Nucléaire/Service d'Expérimentation en Physique Nucléaire, Centre d'Etudes Nucléaires de Saclay, 91191 Gif-sur-Yvette, France*

[2]*Department of Chemistry and Indiana University Cyclotron Facility, Indiana University, Bloomington, Indiana 47405*

[3]*Department of Physics, University of Iowa, Iowa City, Iowa 52242*

(Received 4 March 1991)

Multifragment events for intermediate-mass fragments ($3 \leq Z \leq 12$) with multiplicity up to four have been observed in the reaction of 0.90 and 3.6 GeV ^{3}He ions with ^{nat}Ag nuclei. Fragment energy spectra and angular distributions are found to be dependent on event multiplicity. The data suggest significant modification of the Coulomb field of the emitting source.

PACS numbers: 25.55.−e

Multifragmentation—i.e., final states involving "instantaneous" emission of two or more intermediate-mass fragments (IMF, $3 \leq Z \lesssim Z_{\text{total}}/3$)—is a subject of intensive investigation at the present time. Emulsion studies, plus several coincidence measurements, have demonstrated the existence of multiple-IMF emission at bombarding energies in excess of the total nuclear binding energy [1–5]. In addition, systematic measurements of complex-fragment emission in energetic light-ion-induced reactions have indicated important changes in the mechanism of IMF formation at energies above about 1 GeV [6–9]. Whether the observed multifragment results are the consequence of sequential statistical binary decays or represent an instantaneous breakup of nuclear matter remains an important unresolved question [10]. The important objective of searches for instantaneous multifragmentation is to understand the response of nuclear matter to extreme conditions of temperature and pressure, thereby shedding light on the nuclear equation of state [11,12]. Of related interest are questions of excitation energy deposition on a fast time scale and collective flow effects associated with transverse momentum transfer.

In this Letter we report experimental data from multifold coincidence studies of IMFs emitted in the bombardment of ^{nat}Ag nuclei with 0.90 and 3.6 GeV ^{3}He ions at the Laboratoire Nationale Saturne. Complete excitation function data now exist for this system up to 3.6 GeV [8,13,14]. These studies have indicated a change in the character of IMF emission at bombarding energies just above the total binding energy of this system, i.e., above about 1 GeV. This conclusion is based on the following observations [8]: (1) IMF cross sections increase strongly as a function of bombarding energy, especially at backward angles; (2) changes are observed in the shapes of the fragement kinetic-energy spectra in which the high-energy tails become much harder and the Coulomb peaks are significantly broadened toward lower fragment energies; and (3) a saturation occurs in the fragment charge distributions, $\sigma(Z) = \alpha Z^{-\tau}$, in which the exponent τ becomes constant at $\tau = 2.1 \pm 0.1$. These features are similar to the results of previous inclusive studies of IMF emission in the p+Xe reaction [6].

In the present experiment high-purity, self-supporting ^{nat}Ag targets of thickness 900 μg/cm^2 and area 20 cm^2 were bombarded with ^{3}He ions of energies 0.90 and 3.6 GeV. Beam intensities, about 10^9 particles/s, were monitored by a secondary emission monitor (SEM); absolute normalizations were determined by irradiating carbon targets and using known cross sections [15] for the ^{11}C radioactivity produced by a given integral flux in the SEM. The absolute normalization error for the cross sections quoted here is estimated to be about 30%.

An array of 36 particle-identification telescopes that covered 8% of the total solid angle was employed in these studies. A global array of 32 telescopes was arranged in eight units of area 10×10 cm^2, each consisting of four 5×5 cm^2 detector elements. This provided approximately random sampling of the 4π solid angle. Each quad unit was mounted on one of the three rings oriented at central angles of 35°, 63°, and 117° with respect to the beam axis. Typical target-detector distances were 25–30 cm. Units on a given ring were separated by 120° in azimuthal angle; each ring was offset by 40° with respect to each of the other two rings. Each telescope in the array consisted of an axial-field gas-ionization chamber of length 6 cm operated at 20 Torr of CF_4, followed by a 500-μm-thick ion-implanted passivated silicon detector [Si(IP)] of area 25 cm^2. In addition, four telescopes were mounted in a planar configuration at angles of 25°, 63°, 107°, and 149°. These consisted of similar gas-ionization chambers, followed by 200 μm and 300–500 μm Si(IP) detectors, and a CsI(Tl) crystal capable of stopping 70-MeV/nucleon light charged particles [16]. Event trigger logic permitted data to be recorded as either separate singles IMF events or any combination of IMF coincidences.

One of the primary objectives of this study was to examine multifragment emission at bombarding energies just below and well above threshold in light-ion-induced reactions, as suggested by previous studies [2,6,8]. In

Fig. 1(a) we show the average differential cross sections as a function of observed coincidences ($M_{\mathrm{IMF}}^{\mathrm{obs}}$) for IMFs directly measured in this work. The range of IMF charge acceptance is $Z=3$–12, and the solid angle for the full 36-detector array is 1.0 sr. At both energies the evidence for multiple-fragment events is clear, even with the relatively low solid-angle coverage. In addition to the significant increase in probability for multifragment emission at the higher energy, there is a clear enhancement in the cross section as a function of $M_{\mathrm{IMF}}^{\mathrm{obs}}$ at 3.6 GeV relative to 0.90 GeV. For example, the cross section for $M_{\mathrm{IMF}}^{\mathrm{obs}}=3$ events is over 40 times larger at 3.6 GeV than at 0.90 GeV.

In an effort to assess the effects of detector geometrical acceptance as well as IMF angular distributions on the observed coincidence distributions, base line Monte Carlo simulations have been performed. Two assumptions are included in this simulation: (1) experimental angular distributions for the inclusive IMF yields [8] and (2) an isotropic emission pattern. These values of the reconstructed coincidence distribution ($M_{\mathrm{IMF}}^{\mathrm{rc}}$) are shown in Fig. 1(b) for the data at 0.9 GeV, where these two assumptions diverge most noticeably. This should provide approximate lower limits for the true multiplicity distributions. The reconstructed distributions yield minimum cross sections for multifragment events ($M\geq 2$) of about 220 mb at 3.6 GeV and 20 mb at 0.90 GeV.

To examine the possible sequential nature of the observed multifragment events, calculations were performed with the statistical decay codes EDMON [17] and GEMINI [18]. An average excitation energy of 610 MeV was employed for the postcascade heavy fragments. This value is based on calculations with the ISABEL cascade code [19] for highly central collisions at 3.6 GeV within an impact parameter $b\leq 2.6$ fm which corresponds approximately to the observed cross section for reconstructed multifragment events. Both calculations severely underestimate the multiplicity distributions with self-consistent input values for the cross section and angular momentum distributions.

In Fig. 2 we show the summed IMF charge distributions and the summed IMF kinetic energies for $M_{\mathrm{IMF}}^{\mathrm{obs}}\geq 2$ events. Light charged particles are not included in these sums. At 3.6 GeV bombarding energy events are detected which account for up to 75% of the total available charge—even with only 8% of total solid-angle coverage. Figure 2(a) demonstrates that the observed fragments contain significant contributions from higher-Z fragments (but $Z\leq 12$) and are not exclusively due to light elements such as Li and Be. In addition, the total observed kinetic energy per event extends up to 400 MeV, even with light charged particles excluded from the sums. The solid line in Fig. 2(b) is the result of a calculation based upon sequential statistical emission of IMFs from an equilibrated targetlike source with normal nuclear matter density, initially at a temperature of 8 MeV and corrected for detector acceptance. The simulation assumed as input experimental values for the fragment charge distributions [8] and the reconstructed multiplicity results from Fig. 1. Corrections also were included for the velocity of the emitting source, as determined by rapidity plots based on the singles data. In order to assess the upper limit for fragment kinetic energies, cooling by H and He emission was blocked in this calculation. Even for this

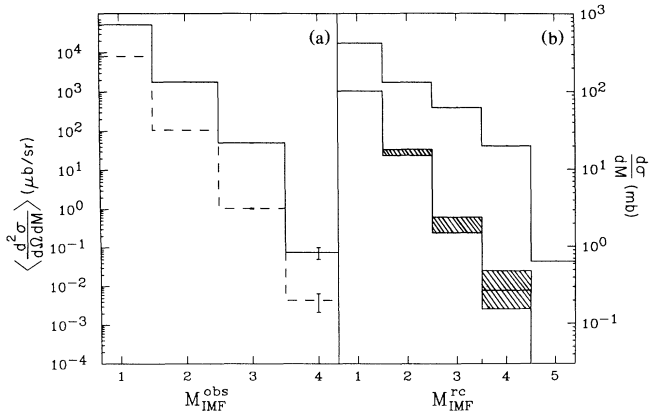

FIG. 1. (a) Differential IMF multiplicities for observed multifragment events measured in the ^{3}He+$^{\mathrm{nat}}$Ag reaction at 900 MeV (dashed line) and 3.6 GeV (solid line). (b) Monte Carlo reconstruction of data in (a) to account for detector geometry. Upper line shows results for 3.6 GeV which assumes singles angular distribution [8]. Lower line is for 0.90 GeV; the cross-hatched area indicates effects of including angular distribution assumptions and statistics.

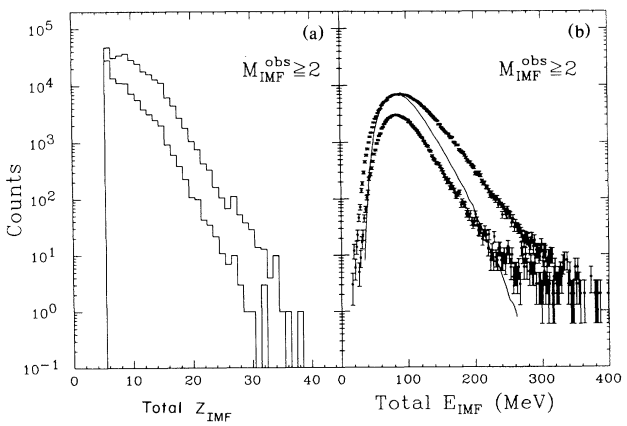

FIG. 2. (a) Distributions of summed IMF charge for IMFs with $M_{\mathrm{IMF}}^{\mathrm{obs}}\geq 2$ for the 3.6 (top) and 0.90 (bottom) GeV ^{3}He+$^{\mathrm{nat}}$Ag reactions. (b) Distributions of summed detected kinetic energy per event for IMFs for $M_{\mathrm{IMF}}^{\mathrm{obs}}\geq 2$ for 3.6 (top) and 0.90 (bottom) GeV. Solid line is result of simulation based on sequential statistical emission, normalized to the peak of the 3.6-GeV data.

extreme assumption, the calculated total kinetic energies fail to approach the experimental distribution, suggesting that the fragment acceleration mechanism is more complex than simple Coulomb repulsion from a thermal source.

Comparison of the summed IMF charge and kinetic-energy distributions for $M \geq 2$ in Fig. 2 reveals qualitatively similar shapes at 900 MeV and 3.6 GeV. This is in contrast to the IMF singles data at these two energies, where distinct changes in the charge distributions and energy spectra have been reported [8]. We interpret this result as due to a major contribution to the IMF singles yields from binary preequilibrium processes at 900 MeV, whereas at 3.6 GeV there is a much higher relative probability for multiple-fragment emission. However, when multifragment events are selected out, as in Fig. 2, the ejectile behavior is similar at both energies.

One of the most distinctive features of our previous inclusive studies [8] was a transition in the shapes of the IMF energy spectra above 1 GeV bombarding energy. References [2] and [6] report similar results for proton-induced reactions. This behavior is examined more quantitatively in Fig. 3, where the kinetic-energy spectra for carbon fragments measured at each of the three angles are shown as a function of $M_{\mathrm{IMF}}^{\mathrm{obs}}$ for both bombarding energies. Here the solid angle is defined by all detectors in a given ring at the specified angle. Similar results are observed for all IMF Z values. Each frame presents spectra gated on $M_{\mathrm{IMF}}^{\mathrm{obs}} = 1$, 2, and 3, respectively, from the entire detector array.

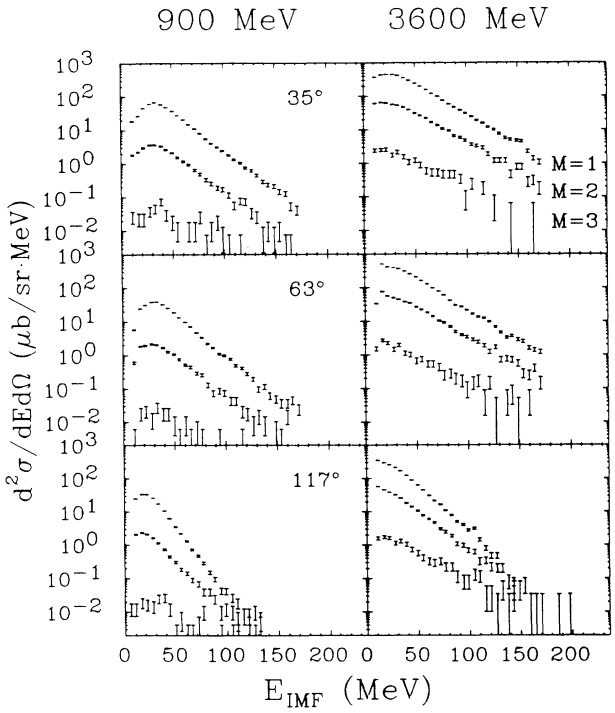

FIG. 3. Energy spectra of carbon fragments for 900 MeV (left column) and 3.6 GeV (right column) observed at 35° (top row), 63° (middle row), and 117° (bottom row). In each frame, top spectrum is for $M_{\mathrm{IMF}}^{\mathrm{obs}} = 1$, middle is for $M_{\mathrm{IMF}}^{\mathrm{obs}} = 2$, and bottom is for $M_{\mathrm{IMF}}^{\mathrm{obs}} = 3$. Errors are statistical, based on total counts.

When the spectra are examined as a function of $M_{\mathrm{IMF}}^{\mathrm{obs}}$, one observes marked changes in which the spectral shapes become increasingly flat with increasing multiplicity. This is most apparent in the backward-angle data. A simple Maxwellian fit to the $\theta = 117°$ spectra at 3.6 GeV gives slope parameters of $T \cong 13$, 15, and 19 MeV for $M_{\mathrm{IMF}}^{\mathrm{obs}} = 1$, 2, and 3, respectively. Similar behavior is exhibited by all other complex fragments. In these fits the Coulomb barriers were much smaller than for touching spheres, suggesting expansion of the source [20] and/or significant charge loss prior to fragment emission. For the 900-MeV data, the spectra for high-$M_{\mathrm{IMF}}^{\mathrm{obs}}$ events are found to be much flatter and exhibit Coulomb peaks which extend to much lower energies than for the singles observations. This is consistent with our interpretation that at an energy of 0.90 GeV, the IMF yield is dominated by binary nonequilibrium emission or statistical decay. At 3.6 GeV the probability for multifragment emission is greatly enhanced, thus masking the spectra of simpler binarylike processes and producing a more isotropic emission pattern.

Another perspective on the influence of multiplicity on reaction observables is illustrated by the rapidity plots shown in Fig. 4. Here we compare invariant cross-section contours as a function of longitudinal and transverse velocity components for carbon fragments emitted in the 3.6-GeV bombardment. For $M_{\mathrm{IMF}}^{\mathrm{obs}} = 1$ (top) the source velocity appears to increase approximately linearly from $v_s \approx 0.4$ to 0.8 cm/ns as a function of IMF velocity. The 0.90-GeV data behave similarly; similar results have been noted in previous inclusive studies [21]. In contrast, for $M_{\mathrm{IMF}}^{\mathrm{obs}} = 3$ (bottom) all the data are described by a single source velocity, $v_s \approx 0.4$ cm/ns. This result implies that the reaction mechanism associated with these high-multiplicity events may be distinctly different from a simple sequential decay process. Clearly, data of a 4π character and realistic model calculations are required to test this assertion quantitatively.

Finally, comparison of the spectra at the two bombarding energies in Fig. 3 shows that at 3.6 GeV the Coulomb peaks are systematically broadened toward lower fragment energies and the spectral tails are much harder. This behavior indicates that for IMF emission above a bombarding energy of ~ 1 GeV, the properties of the emitting source are significantly modified relative to the situation at lower energies. This is especially pronounced when IMFs are observed in the backward-angle detectors. It is also consistent with a picture in which the most violent events are selected when IMFs are observed at backward angles.

In summary, these coincidence experiments have demonstrated the existence of multifragment emission

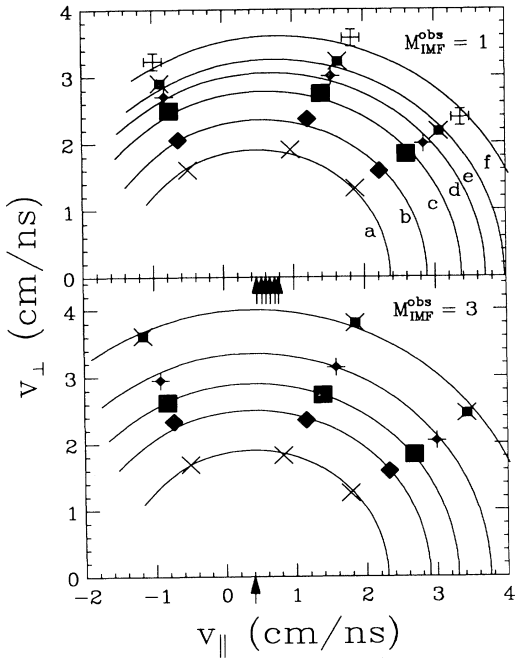

FIG. 4. Invariant cross sections for carbon fragments produced in the 3.6 GeV ^{3}He+^{nat}Ag reaction. Top: Fragments gated on $M_{IMF}^{obs}=1$; arrows are source-velocity centroids of best-fit contour lines through the data, labeled sequentially a,b,c,d,e,f. Bottom: Fragments gated on $M_{IMF}^{obs}=3$; arrow is source-velocity centroid for all contour lines.

with up to four coincident IMFs per event in the ^{3}He $+^{nat}$Ag reaction. The fragment multiplicities are much larger than predicted by statistical emission codes. The summed IMF charge distributions demonstrate that the multifragment yields contain significant contributions from higher-Z fragments, accounting for over 75% of the total charge in some cases. In addition, summed IMF kinetic-energy spectra extend up to 400 MeV, a result which is difficult to reconcile with a sequential statistical decay calculation. The systematic evolution of the fragment kinetic-energy distributions with increasing multiplicity and bombarding energy suggests significant modifications of the Coulomb field of the emitting system. This behavior is consistent with the predictions of the expanding, evaporating source model of Friedman [20], which can also successfully reproduce the multiplicity data. Finally, a rapidity analysis of the data at 3.6 GeV indicates that the high-multiplicity events can be described by a single source, whereas for $M_{IMF}^{obs}=1$, the source velocity increases with increasing IMF energy.

The assistance of the staff at DPhN/BE and LNS in Saclay, and IUCF is gratefully acknowledged, especially that of C. Mazur, J. P. Passérieux, J. Giacometti, G. Milleret, and W. Lozowski. Lai Wan Woo and Erin Renshaw assisted with the calculations. The earlier support of S. Harar is also appreciated. One of us (S.J.Y.) acknowledges the fellowship support of Amoco Corp. This work was supported by DPhN/SEPN, CEN Saclay, the U.S. Department of Energy, and The National Science Foundation. The experiment was performed at the Laboratoire National Saturne.

[a]Present address: Indiana Academy, Ball State University, Muncie, IN 47306.

[1] B. Jakobsson *et al.*, Nucl. Phys. **A488**, 251c (1988).
[2] A. I. Warwick *et al.*, Phys. Rev. C **27**, 1083 (1983).
[3] B. Jacak *et al.*, Nucl. Phys. **A488**, 319c (1988).
[4] R. Trockel *et al.*, Phys. Rev. C **39**, 729 (1989).
[5] Y. Kim *et al.*, Phys. Rev. Lett. **63**, 494 (1989).
[6] N. Porile *et al.*, Phys. Rev. C **39**, 1914 (1989); M. Mahi *et al.*, Phys. Rev. Lett. **60**, 1936 (1988).
[7] G. Klotz-Engmann *et al.*, Phys. Lett. B **187**, 245 (1987); Nucl. Phys. **A499**, 392 (1988).
[8] S. J. Yennello *et al.*, Phys. Lett. B **246**, 26 (1990).
[9] V. V. Avdeichikov *et al.*, Yad. Fiz. **48**, 1736 (1988) [Sov. J. Nucl. Phys. **48**, 1043 (1988)].
[10] W. A. Friedman, Phys. Rev. C **40**, 2055 (1989).
[11] W. G. Lynch, Annu. Rev. Nucl. Sci. **37**, 493 (1987).
[12] *Proceedings of the Symposium on Nuclear Dynamics and Nuclear Disassembly,* edited by J. B. Natowitz (World Scientific, Singapore, 1989).
[13] L. G. Sobotka *et al.*, Phys. Rev. Lett. **51**, 2187 (1983).
[14] K. Kwiatkowski *et al.*, Phys. Lett. B **171**, 41 (1986).
[15] H. Quechon, Ph.D. thesis, University of Paris-Sud, Orsay, 1980 (unpublished).
[16] K. Kwiatkowski *et al.*, Nucl. Instrum. Methods Phys. Res., Sect. A **299**, 166 (1990).
[17] F. Auger *et al.*, Phys. Rev. C **35**, 190 (1987); J. P. Wieleczko (private communication).
[18] R. Charity *et al.*, Nucl. Phys. **A483**, 371 (1988).
[19] Y. Yariv and Z. Frankel, Phys. Rev. C **26**, 2138 (1982).
[20] W. A. Friedman, Phys. Rev. C **42**, 667 (1990).
[21] R. E. L. Green and R. G. Kerteling, Phys. Rev. C **22**, 1594 (1980).